



Observation of lower
tropospheric ozone
enhancement over
East Asia

S. Hayashida et al.

This discussion paper is/has been under review for the journal Atmospheric Chemistry and Physics (ACP). Please refer to the corresponding final paper in ACP if available.

Observation of ozone enhancement in the lower troposphere over East Asia from a space-borne ultraviolet spectrometer

S. Hayashida¹, X. Liu², A. Ono¹, K. Yang^{3,4}, and K. Chance²

¹Faculty of Science, Nara Women's University, Nara, 630-8263, Japan

²Harvard-Smithsonian Center for Astrophysics, Cambridge, Massachusetts, 02138, USA

³Department of Atmospheric and Oceanic Science, University of Maryland College Park, Maryland, 20742, USA

⁴NASA Goddard Space Flight Center, Greenbelt, Maryland, 20771, USA

Received: 13 November 2014 – Accepted: 31 December 2014 – Published: 22 January 2015

Correspondence to: S. Hayashida (sachiko@ics.nara-wu.ac.jp)

Published by Copernicus Publications on behalf of the European Geosciences Union.

Title Page

Abstract

Introduction

Conclusions

References

Tables

Figures



Back

Close

Full Screen / Esc

Printer-friendly Version

Interactive Discussion



Abstract

We report observations from space using ultraviolet (UV) radiance for significant enhancement of ozone in the lower troposphere over Central and Eastern China (CEC). The recent retrieval products of the Ozone Monitoring Instrument (OMI) onboard the Earth Observing System (EOS)/Aura satellite revealed the spatial and temporal variation of ozone distributions in multiple layers in the troposphere. We compared the OMI-derived ozone over Beijing with airborne measurements by the Measurement of Ozone and Water Vapor by Airbus In-Service Aircraft (MOZAIC) program. The correlation between OMI and MOZAIC ozone in the lower troposphere was reasonable, which assured the reliability of OMI ozone retrievals in the lower troposphere under enhanced ozone conditions. The ozone enhancement was clearly observed over CEC, with Shandong Province as its center, and most notable in June in any given year. Similar seasonal variations were observed throughout the nine-year OMI measurement period of 2005 to 2013. The ozone enhancement in June was associated with the enhancement of carbon monoxide (CO) and hotspots, which is consistent with previous studies of in-situ measurements such those made by the MTX2006 campaign. A considerable part of this ozone enhancement could be attributed to the emissions of ozone precursors from open crop residue burning (OCRB) after the winter wheat harvest, in addition to emissions from industrial activities and automobiles. The ozone distribution presented in this study is also consistent with some model studies that apply emissions from OCRB. The lower tropospheric ozone distribution is first shown from OMI retrieval in this study, and the results will be useful in clarifying any unknown factors that influence ozone distribution by comparison with model simulations.

Observation of lower tropospheric ozone enhancement over East Asia

S. Hayashida et al.

Title Page

Abstract

Introduction

Conclusions

References

Tables

Figures



Back

Close

Full Screen / Esc

Printer-friendly Version

Interactive Discussion



1 Introduction

Ozone in the atmospheric boundary layer is produced by chemical reactions between nitrogen oxides (NO_x) and volatile organic compounds (VOCs) in the presence of sunlight. Anthropogenic activities contribute to atmospheric concentrations of NO_x and VOCs, and the resulting boundary layer ozone has harmful effects on plant growth and human health. The ozone produced in the boundary layer is transported to the free troposphere and is dispersed globally. Since ozone absorbs infrared earth radiation, increased ozone contributes to global warming. In the Fourth Assessment Report of the Intergovernmental Panel on Climate Change (IPCC AR4; IPCC, 2007), the contribution of the tropospheric ozone increase after the Industrial Revolution to global warming was estimated to be 0.25 to 0.65 W m⁻² in terms of radiative forcing for the years 1750 to 2005.

In recent years, ozone pollution has become a serious environmental problem in megacities around the world, and the hazardous air pollution over large cities in China is particularly concerning. Thus far, many studies conducted with ground-based measurements have reported significant enhancements in ozone concentrations near the surface over Beijing (e.g. Wang et al., 2006) and the North China Plain (e.g. Lin et al., 2008; Ding et al., 2013). Emissions of ozone precursors from industrial activities and automobile exhaust have been examined to understand the air pollution over China, and a comprehensive bottom-up emission inventory has been developed (Streets et al., 2003; Ohara et al., 2007). However, recent studies have shown that agricultural activities such as open crop residue burning (OCRB) may also have a significant effect on ozone pollution over the North China Plain (Fu et al., 2007; Kanaya et al., 2013). The inclusion of OCRB in the bottom-up inventory is currently a major research topic (Yamaji et al., 2010), although emissions of ozone precursors from agricultural activities have been difficult to quantify. Direct ozone monitoring can yield more important information than that derived from the indirect monitoring of ozone precursors to evaluate the actual extent of ozone pollution. However, the surface ozone-monitoring

ACPD

15, 2013–2054, 2015

Observation of lower tropospheric ozone enhancement over East Asia

S. Hayashida et al.

Title Page

Abstract

Introduction

Conclusions

References

Tables

Figures



Back

Close

Full Screen / Esc

Printer-friendly Version

Interactive Discussion



cur over Central and Eastern China (CEC). Moreover, significant information can be obtained from the retrievals when accumulated in large numbers.

In this study, we present results of the analysis of lower tropospheric ozone over the CEC on the basis of OMI ozone profiles derived from UV radiances. In Sect. 2, we describe the details of the data used in the analysis. In Sect. 3, we show the ozone retrievals and introduce subsequent analyses. In Sect. 4, we discuss the uncertainties involved with ozone retrieval from UV spectra and the possible effects of OCRB on ozone enhancement. In addition, we recommend areas for future research.

2 Data and methodology

2.1 Ozone profile data derived from OMI

OMI is a Dutch-Finnish-built nadir-viewing pushbroom UV/visible instrument carried on National Aeronautics and Space Administration's (NASA's) EOS Aura spacecraft in a sun-synchronous orbit with an equatorial crossing time of $\sim 13:45$ local time (LT). The instrument measures backscattered radiances in three channels covering a wavelength range of 270 to 500 nm (UV-1: 270 to 310 nm; UV-2: 310 to 365 nm; visible: 350 to 500 nm) at a spectral resolution of 0.42 to 0.63 nm (Levelt et al., 2006). OMI has daily global coverage with a spatial resolution of $13 \times 24 \text{ km}^2$ (along and across track) at the nadir position for UV-2 and visible channels and $13 \times 48 \text{ km}^2$ for the UV-1 channel.

Recently, Liu et al. (2010a) developed a new retrieval algorithm for OMI based on that initially developed for GOME (Liu et al., 2005) by using the optimal estimation technique (Rodgers, 2000). They retrieved ozone profiles from the ground upward to about 60 km into 24 layers, of which layers 3–7 are in the troposphere. The lowermost layer, the 24th layer, corresponds to a layer from 0 to about 3 km above the surface. The 23rd and 22nd layers correspond to those about 3 to 6 km and 6 to 8 km in altitude, respectively. However, there is a wide variety of the boundary altitudes depending on meteorological conditions. To constrain the retrievals, Liu et al. (2010a) used climatological mean

Observation of lower tropospheric ozone enhancement over East Asia

S. Hayashida et al.

Title Page

Abstract

Introduction

Conclusions

References

Tables

Figures



Back

Close

Full Screen / Esc

Printer-friendly Version

Interactive Discussion



Observation of lower tropospheric ozone enhancement over East Asia

S. Hayashida et al.

Title Page

Abstract

Introduction

Conclusions

References

Tables

Figures



Back

Close

Full Screen / Esc

Printer-friendly Version

Interactive Discussion



ozone profiles and standard deviations derived from 15 years of ozonesonde measurements and the Stratospheric Aerosol and Gas Experiment (SAGE) as a priori, which varied with latitude and month (McPeters et al., 2007). Several modifications have been made in producing the ozone profile product used in this study, as described by Kim et al. (2013). The retrieval was performed here at a nadir resolution of 52 km \times 48 km by co-adding 4/8 UV1/UV2 pixels to increase the processing speed. In addition, a minimum measurement error of 0.2 % has been imposed in the spectral region of 300 to 330 nm to stabilize the retrievals, although this inclusion also significantly reduced the retrieval sensitivity to lower tropospheric ozone reflected in the retrieval averaging kernels (AKs) compared with those reported by Liu et al. (2010a). However, the reported retrieval sensitivity to tropospheric ozone might be underestimated, because the relative fitting residuals in UV2 (310–330 nm) are generally significantly smaller than 0.2 % and can be as low as 0.06 % except for solar zenith angle greater than 60°.

Here, we show the analysis based on the Level 3 products that are gridded to 1° \times 1° (latitude \times longitude) spatial resolution on a daily basis. The quality of OMI measurements has been impacted by the row anomaly (<http://www.knmi.nl/omi/research/product/rowanomaly-background.php>) that became significant in January 2009, affecting more than one-third of the across-track OMI pixels. OMI pixels affected by the row anomaly were not used in the gridding. The gridded data were screened by the criteria of effective cloud fraction (ECF) $<$ 0.2 and RMS defined as the root mean square of the ratio of fitting residual to assumed measurement error of the UV2 channel $<$ 2.4. The RMS values of OMI retrievals increased with time, especially after 2008. In addition, OMI lost significant spatial coverage due to the row anomaly. A relaxed RMS threshold of 2.4 was used throughout the measurement period to obtain sufficient OMI data for analysis after 2008. Although a stricter threshold was applicable for the period before 2008, this relaxation did not affect data selection because the RMS of most of the data was much smaller ($<$ \sim 1.5) for data before 2008 (Fig. S.1 in the Supplement).

Because the a priori data were taken from climatology and were dependent on latitude and month, seasonal variation must be considered. To follow the temporal evo-

Observation of lower tropospheric ozone enhancement over East Asia

S. Hayashida et al.

Title Page

Abstract

Introduction

Conclusions

References

Tables

Figures

◀

▶

◀

▶

Back

Close

Full Screen / Esc

Printer-friendly Version

Interactive Discussion



lution of the ozone concentration, we analyzed the anomaly of ozone (ΔO_3), which is defined as the difference from the a priori values ($\Delta O_3 = O_3[\text{retrieval}] - O_3[\text{a priori}]$). The ΔO_3 value can be interpreted as an indicator of the ozone variation from OMI measurements regardless of a priori data. It should be noted that the climatological a priori data do not include any significant longitudinal pattern over the regions of focus in this study, although the a priori ozone shows some slight longitudinal variation due to variations in surface and tropopause pressure and thus the thickness of the layer.

2.2 Airborne measurements and ozonesonde measurements over Beijing

The Measurement of Ozone and Water Vapor by Airbus In-Service Aircraft (MOZAIC) program was initiated in 1993 by European scientists, aircraft manufacturers, and airlines to collect experimental data (Marenco et al., 1998). Ozone profiles are obtained during the ascent and descent of aircraft over major cities. Over Beijing, data are available from March 1994 to November 2005 (<http://www.meteo.fr/cic/meetings/2014/MOZAIC-IAGOS/>), and we have archived all profiles. In this study, we used the MOZAIC ozone profiles obtained in 2004 and 2005 to validate the OMI retrieval product in the lower troposphere.

2.3 Meteorological data (NCEP)

Meteorological reanalysis data provided by the National Centers for Environmental Prediction (NCEP; <http://www.esrl.noaa.gov/psd/data/gridded/data.ncep.reanalysis.html>) were used to investigate the meteorological conditions. Pressure height and wind data were utilized to determine the subtropical jet location.

2.4 Hotspots

The biomass burnings detected by satellite observations are expressed as hotspot numbers. Here, we used the hotspot numbers from the global Moderate Resolution Imaging Spectroradiometer (MODIS) Collection 5 active fire product (MCD14ML) as a

3.1.1 Climatology of ozone profiles over Beijing observed by MOZAIC airborne measurements

Ozone profiles over Beijing have been obtained by MOZAIC airborne measurements taken from March 1995 through November 2005. We fully analyzed the ozone profiles over Beijing for the entire period, and here we present the data in 2004 and 2005 when OMI data are also available. Figure 1a shows the daily values of the ozone mixing ratio (in ppbv) observed by MOZAIC measurements over Beijing in 2004 and 2005, and Fig. 1b shows their monthly mean values. For most days, measurements were conducted twice daily; the daily averaged values for the two measurements are shown in Fig. 1a. Numbers of the data used for each month are shown in Fig. 1b. Some profiles do not cover all altitudes, as shown in the figure; thus, the numbers of the data depended on altitude for some months. Above 6 km in altitude, the mixing ratio was often as high as 80 to 100 ppbv, as shown in July 2005, which clearly indicates the effects of stratospheric ozone intrusion. During the period of March 1995 to November 2005, we found that the effects of ozone intrusion from the stratosphere were sometimes remarkable over Beijing. Ozone sonde measurements revealed similar features over Sapporo and Tsukuba in winter and early spring every year (Nakatani et al., 2012). In June 2005 enhancement of the lower tropospheric ozone (< 2 km) was remarkable. Because the minimum ozone mixing ratio was also clearly detected at around 4 km in altitude, we concluded that enhancement of the lower tropospheric ozone was not connected to stratospheric ozone intrusion into the lower troposphere. Rather, the ozone enhancement can be regarded as being derived from ozone production in the lower troposphere. A typical example is shown in greater detail in the following section.

3.1.2 A typical example of significant enhancement of lower tropospheric ozone observed on 22 June 2005

Figure 2 depicts the MOZAIC ozone profile obtained at 14:18 LT on 22 June 2005, which is close to the time of OMI observation at 13:45. A significant enhancement

Observation of lower tropospheric ozone enhancement over East Asia

S. Hayashida et al.

Title Page

Abstract

Introduction

Conclusions

References

Tables

Figures



Back

Close

Full Screen / Esc

Printer-friendly Version

Interactive Discussion



Observation of lower tropospheric ozone enhancement over East Asia

S. Hayashida et al.

Title Page

Abstract

Introduction

Conclusions

References

Tables

Figures

◀

▶

◀

▶

Back

Close

Full Screen / Esc

Printer-friendly Version

Interactive Discussion



almost 50 % of the ozone enhancement from the bottom layer can be retrieved. The columns of AKs indicate that retrieval response to the actual enhancement of ozone at 24th layer does not necessarily peak at the 24th layer, but also at upper layers. However, the enhancement of ozone at upper troposphere such as that at the 21st or 22nd layer does not lead to a peak at the 23rd or 24th layer. Therefore, identification of the peak layer of the ozone profile in the OMI retrieval is useful for distinguishing the cause of ozone enhancement.

In the rightmost panels of Fig. 3, we show the correlation between $X - X_a$ (MOZAIC) at the 24th layer and the ΔO_3 (OMI) of the 22nd layer (c1), or the ΔO_3 (OMI) of the 23rd layer (c2). These two panels show better correlation than that with the same layer as in (b2) and (b3), which indicates that the effect of enhancement of ozone at the 24th layer could propagate to the upper layers. In panel (c3), we also show the correlation between $X - X_a$ (MOZAIC) at the 24th layer and the summation of ΔO_3 (OMI) of the 23rd layer and of the 24th layer.

To confirm the consistency in the OMI ozone retrievals, we applied OMI AKs (rows) to the MOZAIC data by using the following equation:

$$X'_j = X_{a,j} + \sum_{i=1}^n A(i, j) [X_{t,i} X_{a,i}], \quad (1)$$

where X'_j is the MOZAIC ozone profile convolved with the retrieval AKs ($A(i, j)$), X_t is the MOZAIC ozone profile on the OMI altitude grid, and X_a is the a priori profile used in the OMI retrievals. Here, $n = 24$, and $j = 24$ for the 24th layer of the OMI ozone. We applied Eq. (1) to MOZAIC measurements only for $i = 22, 23$, and 24 , and we assumed X_t as the OMI-retrieved data for the other layers above ($i = 1, 21$) because of the unavailability of measurement data. The ozone values (X_t) on 22 June 2014 are shown in the left panel of Fig. 4.

After applying Eq. (1), we compared the MOZAIC and OMI-retrieved ozone for the 22nd, 23rd, and 24th layers for the 36 days. The leftmost three panels of Fig. 5a1, a2, and a3 show the scatter plots of MOZAIC and OMI ozone retrievals. All data for the

global map of NCEP wind at 200 hPa on the same day with the location of the maximum wind speed indicating STJ. Over the CEC the layer peaks appeared at the 24th layer, which demonstrates that the ozone enhancement occurred in the lower troposphere over CEC rather than in the upper troposphere. We will discuss relationships between ΔO_3 and STJ in Sect. 4.

3.3 Correlation with MOPITT CO and MODIS hotspots over East Asia

In this section, we present relationships between the lower tropospheric ozone enhancements and biomass burning activity. As described in Sect. 1, recent studies have revealed a significant effect of OCRB after the harvest of winter wheat on ozone production in June over the CEC (Kanaya et al., 2013). In Fig. 9, we show East Asian maps of the a priori values, ΔO_3 , and retrieved ozone observed by OMI in the 22nd layer, 23rd layer, and 24th layer on 22 June 2005. The ozone enhancement was clearly visible over Shandong and the North China Plain. For comparison with lower tropospheric ozone enhancements, we also show in Fig. 10a and c the CO distribution observed from MOPITT and the hotspot numbers taken from MODIS obtained on the same day, respectively. The areas in which significant hotspots were found correspond to CO and ozone enhancements. This result obtained from OMI is consistent with that in previous studies of MTX2006 that investigated the effect of OCRB on ozone production. This fact indirectly confirms the validity of OMI products.

3.4 Annual and inter-annual variation of ozone distribution in the lower troposphere

Figure 11 shows the monthly mean value of the OMI-retrieved ozone from January to December 2005 at the 24th layer. It should be noted that the monthly mean map shown in Fig. 11 is not synoptic; rather, it is a composite of patchy measurements made under clear-sky conditions only. However, more than half (> 15) of the data were generally available in most of the areas; the data numbers are shown in the Supplement (Fig. S2).

Observation of lower tropospheric ozone enhancement over East Asia

S. Hayashida et al.

Title Page

Abstract

Introduction

Conclusions

References

Tables

Figures

◀

▶

◀

▶

Back

Close

Full Screen / Esc

Printer-friendly Version

Interactive Discussion



Observation of lower tropospheric ozone enhancement over East Asia

S. Hayashida et al.

[Title Page](#)[Abstract](#)[Introduction](#)[Conclusions](#)[References](#)[Tables](#)[Figures](#)[◀](#)[▶](#)[◀](#)[▶](#)[Back](#)[Close](#)[Full Screen / Esc](#)[Printer-friendly Version](#)[Interactive Discussion](#)

Figure 11 shows obvious ozone enhancement in the lower troposphere in June. The layer peak data were also investigated in June 2005. The most frequent layer peak in June 2005 occurred in the 24th layer over the CEC. This result supports that the ozone enhancement observed in June, other than the typical example day of 22 June, can be attributed to the lower troposphere and not to the upper troposphere. The results shown in Fig. 11f are comparable with those in Fig. 10b and d, and the region of ozone enhancement is also strongly connected to CO and hotspots on a monthly basis.

Figure 12 shows the monthly mean value of the retrieved ozone at the 24th layer in June from 2005 through 2013. The year-to-year variability is significant; however, the spatial distribution pattern is similar every year, whereby a region of high ozone concentration appears around the Shandong Peninsula. The maps after 2009 had relatively noisy features due to inferior data quality and reduced spatial coverage after the severe row anomaly problem in 2009. However, despite some noisy patterns shown in the maps after 2009, the characteristic feature of ozone enhancement can be recognized every year. The data numbers shown in the Supplement (Fig. S3) reveal that most of the grid are covered by more than 15 data.

4 Discussion

4.1 Sensitivity of the OMI ozone retrieval scheme to the lower troposphere

Liu et al. (2010a) reported that although the tropospheric degree of freedom for the signal (DFS) for clear-sky conditions typically peaks in the 500–700 hPa layer (i.e., layer 23) and the DFS in the lower troposphere is generally small, the retrieval efficiency for the lowermost layer is typically 0.4–0.7 for most tropical and mid-latitude summer conditions due to the small solar zenith angles. This indicates that 40–70 % of the actual ozone change from the a priori in the 24th layer can be retrieved although not necessarily at the same layer due to smoothing. For the grid including Beijing shown in Fig. 4, the DFS for layer 24 was only 0.11. However, its AKs for rows (middle panel)

slightly peaked at layer 24, although no significant difference was shown in the lowermost five layers, and the total retrieval efficiency for layer 24 was 0.46.

Although Liu et al. (2010b) also reported validation of OMI ozone profiles between 0.22 and 215 hPa and a stratospheric ozone column decrease to 215 hPa against v2.2 MLS data from 2006, validation for the lowermost altitude has not been sufficiently studied. The validation of OMI ozone retrieval for the lowermost troposphere under conditions of significantly enhanced ozone, such as those observed over the CEC, has not been evaluated prior to this study because only limited ozone profile data over China are available. In this study, we utilized MOZAIC airborne measurement data and examined the possibility of lower tropospheric ozone detection from OMI over Beijing in detail, although the data were limited to the period before November 2005. In Sect. 3.1, we compared the OMI-retrieved ozone data with MOZAIC airborne data over Beijing. We presented in Fig. 2 a typical ozone profile showing significant enhancement in the lower troposphere, and we showed other related results concerning this case.

In addition to the aforementioned case of 22 June 2005, we selected 36 coincident pairs of OMI and MOZAIC data as listed in Table 1, and we compared them in Fig. 3. A direct correlation between the MOZAIC and OMI ozone data showed good linearity, with $R^2 = 0.68$ for the 24th layer (Fig. 3a3). However, the a priori data implicitly involve seasonal variation, and the good correlation shown in Fig. 3a was partly caused by large seasonal variation. Therefore, the observed correlation in Fig. 3a does not assure reliability of OMI ozone retrievals. To avoid this effect on the correlation evaluation, we also showed correlations between the differences from the a priori values, $X - X_a$ and ΔO_3 , in Fig. 3b.

For the lowermost 24th layer, large values of $X - X_a$ (up to 15 DU) were observed by MOZAIC (Fig. 3b3). The OMI retrievals at the 24th layer significantly underestimated the ozone because some of ozone enhancement was retrieved at upper layers, and some could not be retrieved due to reduced photon penetration into the lower troposphere. The regression coefficient of OMI ozone was 0.17 against MOZAIC ozone. On the contrary, the R^2 was as large as 0.47. This linearity of ΔO_3 to $X - X_a$ can be used as

Observation of lower tropospheric ozone enhancement over East Asia

S. Hayashida et al.

Title Page

Abstract

Introduction

Conclusions

References

Tables

Figures



Back

Close

Full Screen / Esc

Printer-friendly Version

Interactive Discussion



Observation of lower tropospheric ozone enhancement over East Asia

S. Hayashida et al.

Title Page

Abstract

Introduction

Conclusions

References

Tables

Figures

◀

▶

◀

▶

Back

Close

Full Screen / Esc

Printer-friendly Version

Interactive Discussion



the high concentrations of O_3 , and its precursors and aerosols, in June was identified as regional-scale OCRB after the harvesting of winter wheat. Kanaya et al. (2013) presented photographs of smoky scenery captured at the observation site. They stated that the composition at the field site was strongly influenced by large-scale post-harvest OCRB of winter wheat.

The ozone enhancement observed in June 2006 by MTX2006 was consistent with the OMI results we presented in this study. We examined a time series of OMI-derived ozone at the grid including that at Mt. Tai ($36.26^\circ N$, $117.11^\circ E$) at the 24th layer during the period of the MTX2006 campaign. Applying the linearity shown in Fig. 3b3, we converted the original OMI retrieval as $\Delta O_3 / 0.17 + X_a$, where 0.17 is the linear regression coefficient. We found that the scale of ozone enhancement up to about 140 ppbv was roughly consistent with that observed in MTX2006, supporting the reliability of the OMI-derived ozone data shown in the present study.

4.4 Suggestions for future study

Ozone enhancement was most notable in June of every year, as presented in Fig. 11. Some model studies were published in the MTX2006 special issue. Li et al. (2008) used a 3-D regional chemical transport model, known as the Nested Air Quality Model System (NAQPMS). They presented the simulated monthly mean near-ground ozone (Fig. 5 of Li et al., 2008), which is comparable to that in Fig. 12b in the present study. Yamaji et al. (2010) used the Model-3 Community Multiscale Air Quality Modeling System (CMAQ) to investigate the effects of OCRB with daily gridded emissions by applying the bottom-up method. They presented daily ozone maps (Fig. 8 of Yamaji et al., 2010), which are also comparable to the OMI daily maps obtained by the present study. The comparison of OMI-derived ozone maps with multiple-mode simulations can lead to a better understanding of emissions from crop burning, which is an important topic for further investigation.

The ozone maps shown in Figs. 11 and 12 indicate that the maximum ΔO_3 value diminished gradually downstream of the CEC, suggesting an outflow of ozone plumes

Observation of lower tropospheric ozone enhancement over East Asia

S. Hayashida et al.

Title Page

Abstract

Introduction

Conclusions

References

Tables

Figures



Back

Close

Full Screen / Esc

Printer-friendly Version

Interactive Discussion



this study because only limited ozone profile data over China are available. We compared the OMI-derived ozone over Beijing with airborne measurements conducted by the MOZAIC program, and we examined in detail the possibility of lower tropospheric ozone detection from OMI over Beijing, although the data were limited to the period before November 2005. Under the condition of highly enhanced ozone such as that over Beijing, the correlation between OMI and MOZAIC ozone in the lower troposphere was reasonable, which verified the reliability of OMI ozone retrievals at the lower troposphere under enhanced ozone conditions. The ozone enhancement over the CEC was clear in June of every year, which is associated with the enhancement of CO and hotspots. This result suggests that a considerable portion of the enhancement could be attributed to the emissions of ozone precursors from residue burning after the harvesting of winter wheat in these regions, as investigated by in-situ measurements in MTX2006 (Kanaya et al., 2013).

The lower tropospheric ozone distribution maps were first obtained from OMI retrieval in the present study; these maps are consistent with the results from some model simulations that include OCRB emissions. The OMI-derived information on lower tropospheric ozone will be helpful for the investigation of as yet unknown factors influencing ozone distribution by comparison with model simulations. Such a topic is intended for future study.

The Supplement related to this article is available online at doi:10.5194/acpd-15-2013-2015-supplement.

Acknowledgements. We express our thanks to the European Commission for the support to the MOZAIC project (1994–2003), to partner institutions of the IAGOS Research Infrastructure (FZJ, DLR, MPI, and KIT in Germany; CNRS, CNES, and Météo-France in France; and the University of Manchester in the United Kingdom), ETHER (CNES-CNRS/INSU) for hosting the database, and to participating airlines (Lufthansa, Air France, Austrian, China Airlines, Iberia, and Cathay Pacific) for transporting the instrumentation free of charge. We also express

our gratitude to Ms. H. Araki and Ms. M. Nakazawa for their help with the data analysis and creation of figures and to Yugo Kanaya for his helpful comments on MTX2006. S. Hayashida and A. Ono were supported by a Grant-in-Aid from the Green Network of Excellence, Environmental Information (GRENE-ei) program, MEXT, Japan. X. Liu and K. Chance were supported by NASA and the Smithsonian Institution.

References

- Aires, F., Aznay, O., Prigent, C., Paul, M., and Bernardo, F.: Synergistic multi-wavelength remote sensing versus a posteriori combination of retrieved products: Application for the retrieval of atmospheric profiles using MetOp-A, *J. Geophys. Res.*, 117, D18304, doi:10.1029/2011JD017188, 2012.
- Chance, K., Palmer, P. I., Spurr, R. J. D., Martin, R. V., Kurosu, T., and Jacob, D. J.: Satellite observations of formaldehyde over North America from GOME, *Geophys. Res. Lett.*, 27, 3461–3464, 2000.
- Cuesta, J., Eremenko, M., Liu, X., Dufour, G., Cai, Z., Höpfner, M., von Clarmann, T., Sellitto, P., Foret, G., Gaubert, B., Beekmann, M., Orphal, J., Chance, K., Spurr, R., and Flaud, J.-M.: Satellite observation of lowermost tropospheric ozone by multispectral synergism of IASI thermal infrared and GOME-2 ultraviolet measurements over Europe, *Atmos. Chem. Phys.*, 13, 9675–9693, doi:10.5194/acp-13-9675-2013, 2013.
- Deeter, M. N., Worden, H. M., Gille, J. C., Edwards, D. P., Mao, D., and Drummond, J. R.: MOPITT multispectral CO retrievals: Origins and effects of geophysical radiance errors, *J. Geophys. Res.*, 116, D15303, doi:10.1029/2011JD015703, 2011.
- Deeter, M. N., Martínez-Alonso, S., Edwards, D. P., Emmons, L. K., Gille, J. C., Worden, H. M., Pittman, J. V., Daube, B. C., and Wofsy, S. C.: Validation of MOPITT Version 5 thermal-infrared, near-infrared, and multispectral carbon monoxide profile retrievals for 2000–2011, *J. Geophys. Res.-Atmos.*, 118, 6710–6725, doi:10.1002/jgrd.50272, 2013.
- Ding, A. J., Fu, C. B., Yang, X. Q., Sun, J. N., Zheng, L. F., Xie, Y. N., Herrmann, E., Nie, W., Petäjä, T., Kerminen, V.-M., and Kulmala, M.: Ozone and fine particle in the western Yangtze River Delta: an overview of 1 yr data at the SORPES station, *Atmos. Chem. Phys.*, 13, 5813–5830, doi:10.5194/acp-13-5813-2013, 2013.

ACPD

15, 2013–2054, 2015

Observation of lower tropospheric ozone enhancement over East Asia

S. Hayashida et al.

Title Page

Abstract

Introduction

Conclusions

References

Tables

Figures

◀

▶

◀

▶

Back

Close

Full Screen / Esc

Printer-friendly Version

Interactive Discussion



Observation of lower tropospheric ozone enhancement over East Asia

S. Hayashida et al.

Title Page

Abstract

Introduction

Conclusions

References

Tables

Figures



Back

Close

Full Screen / Esc

Printer-friendly Version

Interactive Discussion



- Kanaya, Y., Akimoto, H., Wang, Z.-F., Pochanart, P., Kawamura, K., Liu, Y., Li, J., Komazaki, Y., Irie, H., Pan, X.-L., Taketani, F., Yamaji, K., Tanimoto, H., Inomata, S., Kato, S., Suthawaree, J., Okuzawa, K., Wang, G., Aggarwal, S. G., Fu, P. Q., Wang, T., Gao, J., Wang, Y., and Zhuang, G.: Overview of the Mount Tai Experiment (MTX2006) in central East China in June 2006: studies of significant regional air pollution, *Atmos. Chem. Phys.*, 13, 8265–8283, doi:10.5194/acp-13-8265-2013, 2013.
- Kar, J., Fishman, J., Creilson, J. K., Richter, A., Ziemke, J., and Chandra, S.: Are there urban signatures in the tropospheric ozone column products derived from satellite measurements?, *Atmos. Chem. Phys.*, 10, 5213–5222, doi:10.5194/acp-10-5213-2010, 2010.
- Kim, P. S., Jacob, D. J., Liu, X., Warner, J. X., Yang, K., Chance, K., Thouret, V., and Nedelec, P.: Global ozone-CO correlations from OMI and AIRS: constraints on tropospheric ozone sources, *Atmos. Chem. Phys.*, 13, 9321–9335, doi:10.5194/acp-13-9321-2013, 2013.
- Landgraf, J. and Hasekamp, O. P.: Retrieval of tropospheric ozone: The synergistic use of thermal infrared emission and ultraviolet reflectivity measurements from space, *J. Geophys. Res.*, 112, D08310, doi:10.1029/2006JD008097, 2007.
- Levelt, P. F., van den Oord, G. H. J., Dobber, M. R., Malkki, A., Huib, V., Johan de, V., Stammes, P., Lundell, J. O. V., and Saari, H.: The Ozone Monitoring Instrument, *IEEE T. Geosci. Remote*, 44, 1093–1101, doi:10.1109/tgrs.2006.872333, 2006.
- Li, J., Wang, Z., Akimoto, H., Yamaji, K., Takigawa, M., Pochanart, P., Liu, Y., Tanimoto, H., and Kanaya, Y.: Near-ground ozone source attributions and outflow in central eastern China during MTX2006, *Atmos. Chem. Phys.*, 8, 7335–7351, doi:10.5194/acp-8-7335-2008, 2008.
- Lin, W., Xu, X., Zhang, X., and Tang, J.: Contributions of pollutants from North China Plain to surface ozone at the Shangdianzi GAW Station, *Atmos. Chem. Phys.*, 8, 5889–5898, doi:10.5194/acp-8-5889-2008, 2008.
- Liu, X., Chance, K., Sioris, C. E., Spurr, R. J. D., Kurosu, T. P., Martin, R. V., and Newchurch, M. J.: Ozone profile and tropospheric ozone retrievals from the global ozone monitoring experiment: Algorithm description and validation, *J. Geophys. Res.*, 110, D20307, doi:10.1029/2005JD006240, 2005.
- Liu, X., Bhartia, P. K., Chance, K., Spurr, R. J. D., and Kurosu, T. P.: Ozone profile retrievals from the Ozone Monitoring Instrument, *Atmos. Chem. Phys.*, 10, 2521–2537, doi:10.5194/acp-10-2521-2010, 2010a.
- Liu, X., Bhartia, P. K., Chance, K., Froidevaux, L., Spurr, R. J. D., and Kurosu, T. P.: Validation of Ozone Monitoring Instrument (OMI) ozone profiles and stratospheric ozone columns

Observation of lower tropospheric ozone enhancement over East Asia

S. Hayashida et al.

Title Page

Abstract

Introduction

Conclusions

References

Tables

Figures



Back

Close

Full Screen / Esc

Printer-friendly Version

Interactive Discussion



with Microwave Limb Sounder (MLS) measurements, *Atmos. Chem. Phys.*, 10, 2539–2549, doi:10.5194/acp-10-2539-2010, 2010b.

Marenco, A., Thouret, V., Nedelec, P., Smit, H., Helton, M., Kley, D., Karcher, F., Simon, P., Law, K., Pyle, J., Poschmann, G., Wrede, R. v., Hume, C., and Cook, T.: Measurement of ozone and water vapor by Airbus in-service aircraft: The MOZAIC airborne program, An overview, *J. Geophys. Res.*, 103, 25631–25642, 1998.

McPeters, R. D., Labow, G. J., and Logan, J. A.: Ozone climatological profiles for satellite retrieval algorithms, *J. Geophys. Res.*, 112, D05308, doi:10.1029/2005jd006823, 2007.

Nakatani, A., Kondo, S., Hayashida, S., Nagashima, T., Sudo, K., Liu, X., Chance, K., and Hirota, I.: Enhanced mid-latitude tropospheric column ozone over East Asia: Coupled effects of stratospheric ozone intrusion and anthropogenic sources, *J. Meteor. Soc. Jpn*, 90, 207–222, doi:10.2151/jmsj.2012-204, 2012.

Natraj, V., Liu, X., Kulawik, S., Chance, K., Chatfield, R., Edwards, D. P., Eldering, A., Francis, G., Kurosu, T., Pickering, K., Spurr, R., and Worden, H.: Multi-spectral sensitivity studies for the retrieval of tropospheric and lowermost tropospheric ozone from simulated clear-sky geocape measurements, *Atmos. Environ.*, 45, 7151–7165, doi:10.1016/j.atmosenv.2011.09.014, 2011.

Ohara, T., Akimoto, H., Kurokawa, J., Horii, N., Yamaji, K., Yan, X., and Hayasaka, T.: An Asian emission inventory of anthropogenic emission sources for the period 1980–2020, *Atmos. Chem. Phys.*, 7, 4419–4444, doi:10.5194/acp-7-4419-2007, 2007.

Pan, X. L., Kanaya, Y., Wang, Z. F., Komazaki, Y., Taketani, F., Akimoto, H., and Pochanart, P.: Variations of carbonaceous aerosols from open crop residue burning with transport and its implication to estimate their lifetimes, *Atmos. Environ.*, 74, 301–310, doi:10.1016/j.atmosenv.2013.03.048, 2013.

Richter, A., Burrows, J. P., Nuss, H., Granier, C., and Niemeier, U.: Increase in tropospheric nitrogen dioxide over China observed from space, *Nature*, 437, 129–132, doi:10.1038/nature04092, 2005.

Rodgers, C. D.: Inverse methods for atmospheric sounding: Theory and practice, World Scientific Publishing, Singapore, 2000.

Safieddine, S., Clerbaux, C., George, M., Hadji-Lazaro, J., Hurtmans, D., Coheur, P. F., Wespes, C., Loyola, D., Valks, P., and Hao, N.: Tropospheric ozone and nitrogen dioxide measurements in urban and rural regions as seen by IASI and GOME-2, *J. Geophys. Res. Atmos.*, 118, 10555–10566, doi:10.1002/jgrd.50669, 2013.

Observation of lower tropospheric ozone enhancement over East Asia

S. Hayashida et al.

Title Page

Abstract

Introduction

Conclusions

References

Tables

Figures

◀

▶

◀

▶

Back

Close

Full Screen / Esc

Printer-friendly Version

Interactive Discussion



Streets, D. G., Bond, T. C., Carmichael, G. R., Fernandes, S. D., Fu, Q., He, D., Klimont, Z., Nelson, S. M., Tsai, N. Y., Wang, M. Q., Woo, J.-H., and Yarber, K. F.: An inventory of gaseous and primary aerosol emissions in Asia in the year 2000, *J. Geophys. Res.*, 108, 8809, doi:10.1029/2002jd003093, 2003.

5 Wang, T., Ding, A., Gao, J., and Wu, W. S.: Strong ozone production in urban plumes from Beijing, China, *Geophys. Res. Lett.*, 33, L21806, doi:10.1029/2006GL027689, 2006.

Wang, Y., Konopka, P., Liu, Y., Chen, H., Müller, R., Plöger, F., Riese, M., Cai, Z., and Lü, D.: Tropospheric ozone trend over Beijing from 2002–2010: ozonesonde measurements and modeling analysis, *Atmos. Chem. Phys.*, 12, 8389–8399, doi:10.5194/acp-12-8389-2012, 2012.

10 Worden, J., Liu, X., Bowman, K., Chance, K., Beer, R., Eldering, A., Gunson, M., and Worden, H.: Improved tropospheric ozone profile retrievals using OMI and TES radiances, *Geophys. Res. Lett.*, 34, L01809, doi:10.1029/2006GL027806, 2007.

Yamaji, K., Li, J., Uno, I., Kanaya, Y., Irie, H., Takigawa, M., Komazaki, Y., Pochanart, P., Liu, Y., Tanimoto, H., Ohara, T., Yan, X., Wang, Z., and Akimoto, H.: Impact of open crop residual burning on air quality over Central Eastern China during the Mount Tai Experiment 2006 (MTX2006), *Atmos. Chem. Phys.*, 10, 7353–7368, doi:10.5194/acp-10-7353-2010, 2010.

15 Yan, X., Ohara, T., and Akimoto, H.: Bottom-up estimate of biomass burning in mainland China, *Atmos. Environ.*, 40, 5262–5273, doi:10.1016/j.atmosenv.2006.04.040, 2006.

Table 1. List of the data used for comparison of MOZAIC and OMI.

No.	Date (yyyymmdd)	Time of MOZAIC measurements (LT)
1	2004 10 14	12:48
2	2004 10 24	12:52
3	2004 11 15	13:57
4	2004 12 10	14:20
5	2005 03 04	13:58
6	2005 03 09	14:01
7	2005 03 11	14:06
8	2005 03 18	13:57
9	2005 03 25	14:02
10	2005 03 29	11:40
11	2005 04 03	10:38
12	2005 04 28	10:52
13	2005 05 01	10:28
14	2005 05 03	10:30
15	2005 05 08	10:25
16	2005 05 11	13:46
17	2005 05 12	13:54
18	2005 05 15	10:31
19	2005 05 18	13:50
20	2005 05 24	10:35
21	2005 06 10	13:53
22	2005 06 15	14:17
23	2005 06 22	14:18
24	2005 06 23	11:09
25	2005 08 19	14:11
26	2005 08 21	10:41
27	2005 09 04	10:42
28	2005 09 06	10:51
29	2005 09 14	14:03
30	2005 09 18	10:57
31	2005 09 21	14:04
32	2005 10 05	13:46
33	2005 10 19	13:59
34	2005 10 26	13:58
35	2005 10 30	14:28
36	2005 11 11	14:18

Observation of lower tropospheric ozone enhancement over East Asia

S. Hayashida et al.

Title Page

Abstract

Introduction

Conclusions

References

Tables

Figures



Back

Close

Full Screen / Esc

Printer-friendly Version

Interactive Discussion



Observation of lower tropospheric ozone enhancement over East Asia

S. Hayashida et al.

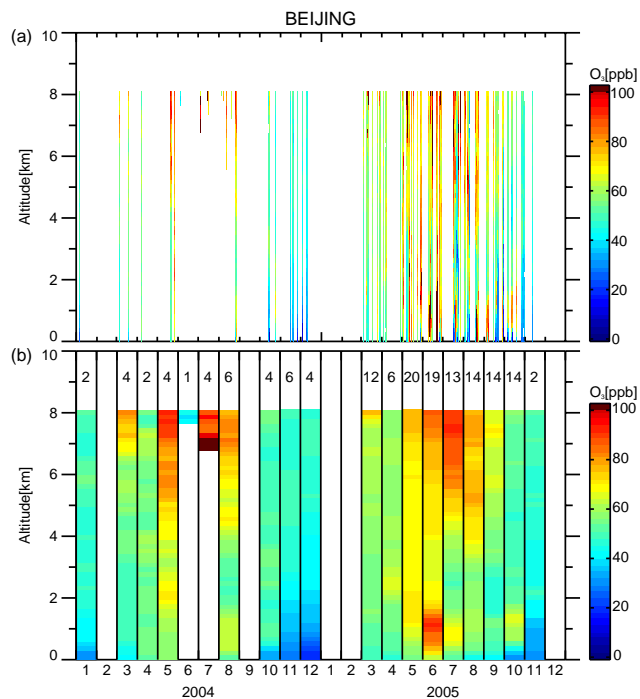


Figure 1. (a) Time–altitude cross section of daily mean ozone mixing ratios observed by MOZAIC over Beijing in 2004 and 2005. Two measurements were conducted on most days. Daily values are the average of the two data sets obtained on the same day. (b) Same as (a) but for monthly mean ozone mixing ratios. The numbers of the data used in the analysis for each month are shown.

Title Page

Abstract

Introduction

Conclusions

References

Tables

Figures

◀

▶

◀

▶

Back

Close

Full Screen / Esc

Printer-friendly Version

Interactive Discussion



Observation of lower tropospheric ozone enhancement over East Asia

S. Hayashida et al.

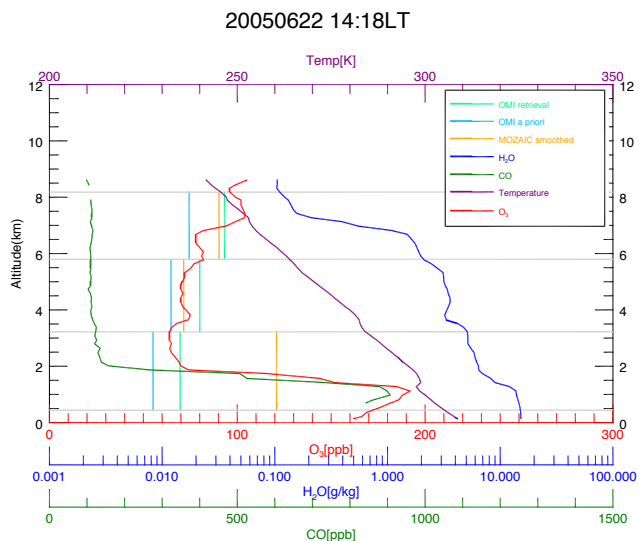


Figure 2. Vertical profiles of ozone (red), CO (green), H₂O (blue), and temperature (purple) obtained by MOZAIC airborne measurements on 22 June 2005 at 14:18 LT over Beijing. The scale of each parameter is shown in the same colors. The smoothed-MOZAIC-ozone profile according to the corresponding OMI layers is shown by orange lines. Correspondingly, a priori and retrieval of OMI are shown in light blue and light green, respectively. The OMI 22nd, 23rd, and 24th layers correspond to 6–8, 3–6, and 0–3 km, respectively.

Title Page

Abstract

Introduction

Conclusions

References

Tables

Figures

◀

▶

◀

▶

Back

Close

Full Screen / Esc

Printer-friendly Version

Interactive Discussion



Observation of lower tropospheric ozone enhancement over East Asia

S. Hayashida et al.

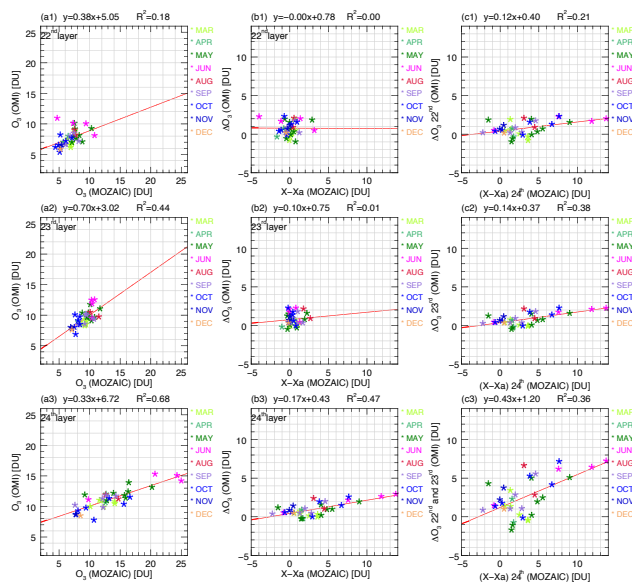


Figure 3. (Left) Direct correlation of MOZAIC ozone data (averaged to adjust for OMI height resolution) and OMI ozone retrievals, at the (a1) 22nd, (a2) 23rd, and (a3) 24th layers for the coincident 36 days in 2004 and 2005. (Middle) Same as leftmost panels but for the differences from a priori values: $X - X_a$ taken from MOZAIC; ΔO_3 taken from OMI. (1), (2), and (3) represent the 22nd, 23rd, and 24th layers, respectively, for the each panel. (Right) Same as in the middle panels but for (c1) $X - X_a$ taken from MOZAIC at the 24th layer and ΔO_3 taken from OMI at the 22nd layer, (c2) $X - X_a$ taken from MOZAIC at the 24th layer and ΔO_3 taken from OMI at the 23rd layer, and (c3) $X - X_a$ taken from MOZAIC at the 24th layer and summation of ΔO_3 taken from OMI at layers 23 and 24. The linear regression equation and coefficient of determination, or R^2 values, are shown above each panel. All data are color-coded according to month. The 36-day data used in the analysis are listed in Table 1.

Title Page

Abstract

Introduction

Conclusions

References

Tables

Figures

◀

▶

◀

▶

Back

Close

Full Screen / Esc

Printer-friendly Version

Interactive Discussion



Observation of lower tropospheric ozone enhancement over East Asia

S. Hayashida et al.

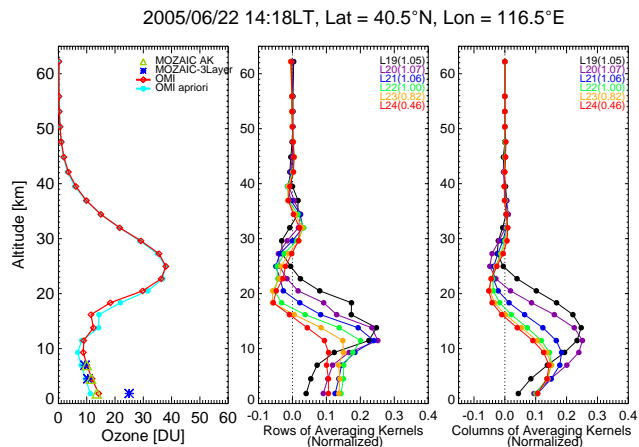


Figure 4. Ozone profile and AKs used for comparison for 22 June 2005. Latitude and longitude correspond to the OMI grid corresponding to the MOZAIC measurements. (Left) Solid blue line indicates OMI a priori ozone profile; solid red line indicates the ozone profile derived from OMI spectra. Blue asterisks indicate MOZAIC ozone values adjusted to corresponding OMI layers. Light green triangles indicate MOZAIC ozone values convolved with the AKs shown in the middle panel. (Middle) Profiles of the rows of AKs normalized by the a priori error for the six layers of OMI retrieval. Black, violet, blue, green, yellow, and red lines correspond to 19th, 20th, 21st, 22nd, 23rd, and 24th layers, respectively. The total retrieval efficiencies are shown in parentheses. (Right) Same as middle panel but for the columns of the AKs normalized by the a priori error.

[Title Page](#)
[Abstract](#)
[Introduction](#)
[Conclusions](#)
[References](#)
[Tables](#)
[Figures](#)
[Back](#)
[Close](#)
[Full Screen / Esc](#)
[Printer-friendly Version](#)
[Interactive Discussion](#)


Observation of lower tropospheric ozone enhancement over East Asia

S. Hayashida et al.

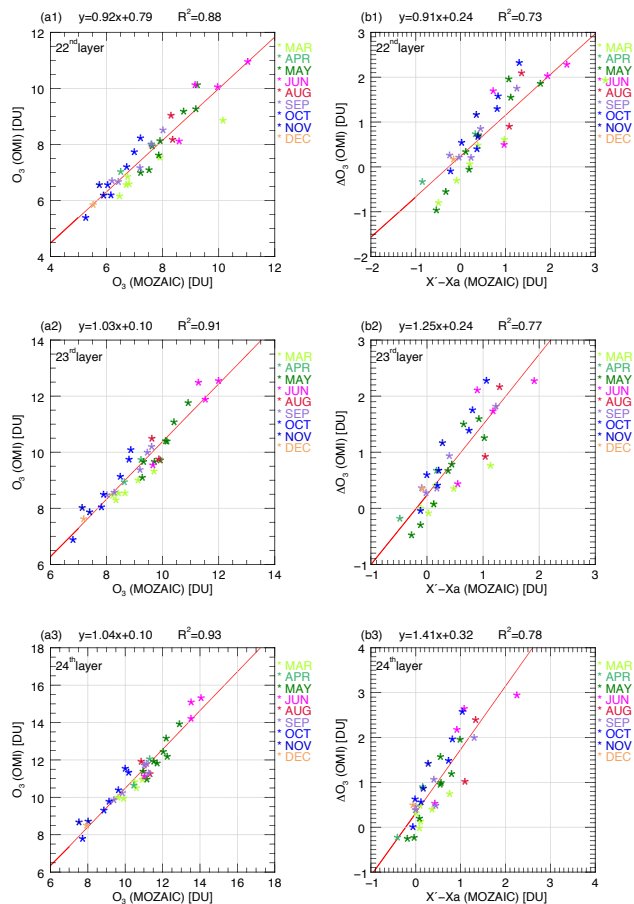


Figure 5. Same as Fig. 3a1–b3 except that MOZAIC values are convolved with OMI Aks (row) according to Eq. (1).

Title Page

Abstract

Introduction

Conclusions

References

Tables

Figures

◀

▶

◀

▶

Back

Close

Full Screen / Esc

Printer-friendly Version

Interactive Discussion



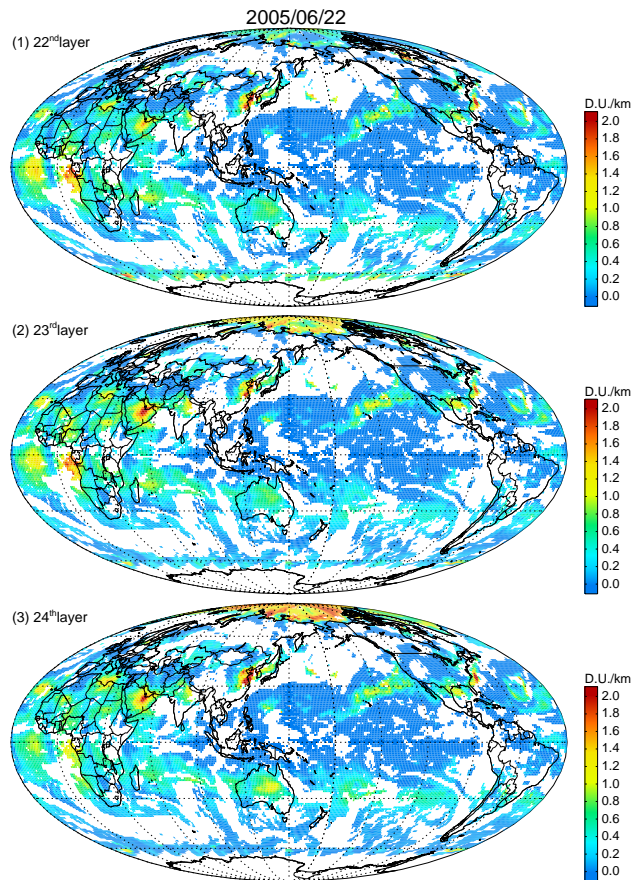


Figure 6. Global maps of ΔO_3 observed by OMI at the (1) 22nd, (2) 23rd, and (3) 24th layer on 22 June 2005, which correspond to the MOZAIC measurement shown in Fig. 2. The unit of ozone amount is noted by $D.U. km^{-1}$. Cloudy areas were screened out with the criteria of $ECF < 0.2$ and data quality as $RMS < 2.4$ (shown in white).

Observation of lower tropospheric ozone enhancement over East Asia

S. Hayashida et al.

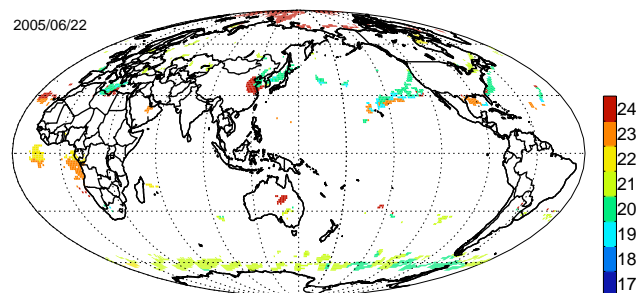


Figure 7. The layer peak for the ozone enhancement (ΔO_3) on 22 June, 2005. Grids were selected where the TCO was larger than 0.8 D.U. km^{-1} .

[Title Page](#)[Abstract](#)[Introduction](#)[Conclusions](#)[References](#)[Tables](#)[Figures](#)[Back](#)[Close](#)[Full Screen / Esc](#)[Printer-friendly Version](#)[Interactive Discussion](#)

Observation of lower tropospheric ozone enhancement over East Asia

S. Hayashida et al.

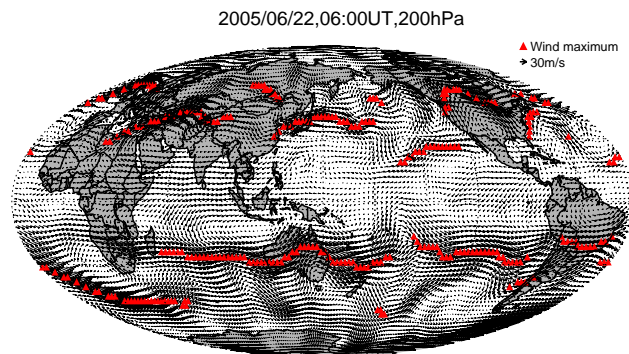


Figure 8. A global map of NCEP wind at 200 hPa at 06:00 UT (14:00 CST). Locations of maximum wind speed along the longitude are denoted by red triangles.

[Title Page](#)[Abstract](#)[Introduction](#)[Conclusions](#)[References](#)[Tables](#)[Figures](#)[Back](#)[Close](#)[Full Screen / Esc](#)[Printer-friendly Version](#)[Interactive Discussion](#)

Observation of lower tropospheric ozone enhancement over East Asia

S. Hayashida et al.

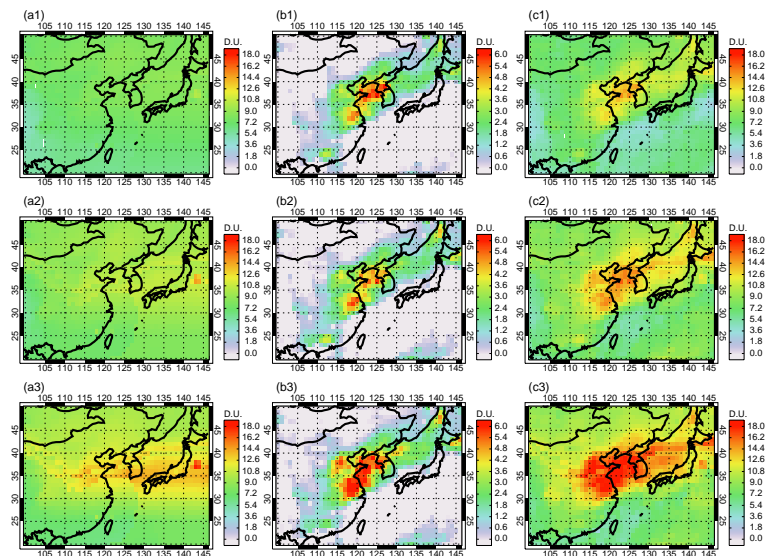


Figure 9. Maps of (a) a priori ozone, (b) OMI-derived ΔO_3 , and (c) OMI-derived O_3 on 22 June 2005. 1, 2, and 3 represent the 22nd, 23rd, and 24th layers, respectively.

[Title Page](#)
[Abstract](#)
[Introduction](#)
[Conclusions](#)
[References](#)
[Tables](#)
[Figures](#)
[Back](#)
[Close](#)
[Full Screen / Esc](#)
[Printer-friendly Version](#)
[Interactive Discussion](#)


Observation of lower tropospheric ozone enhancement over East Asia

S. Hayashida et al.

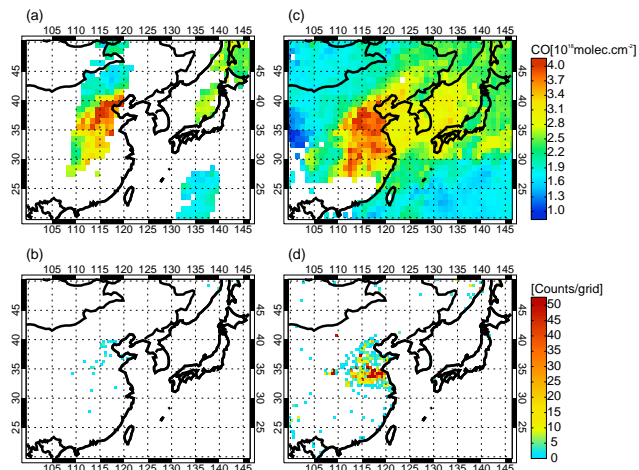


Figure 10. Maps of (a) CO in column number density observed by MOPITT and (b) hotspot numbers taken from MODIS on 22 June 2005 for the grids of $0.5^\circ \times 0.5^\circ$ in latitude and longitude. (c) Same as (a) but for the monthly average of June 2005. (d) Same as (b) but for the monthly accumulation in June 2005.

[Title Page](#)[Abstract](#)[Introduction](#)[Conclusions](#)[References](#)[Tables](#)[Figures](#)[◀](#)[▶](#)[◀](#)[▶](#)[Back](#)[Close](#)[Full Screen / Esc](#)[Printer-friendly Version](#)[Interactive Discussion](#)

Observation of lower tropospheric ozone enhancement over East Asia

S. Hayashida et al.

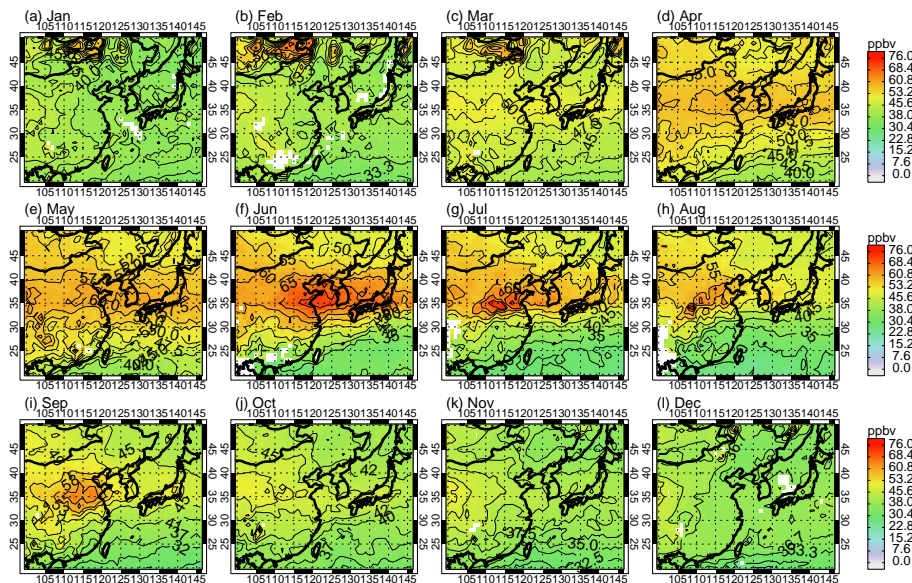


Figure 11. Maps of monthly mean value of retrieved ozone at the 24th layer from January to December 2005.

Title Page

Abstract

Introduction

Conclusions

References

Tables

Figures

◀

▶

◀

▶

Back

Close

Full Screen / Esc

Printer-friendly Version

Interactive Discussion



Observation of lower tropospheric ozone enhancement over East Asia

S. Hayashida et al.

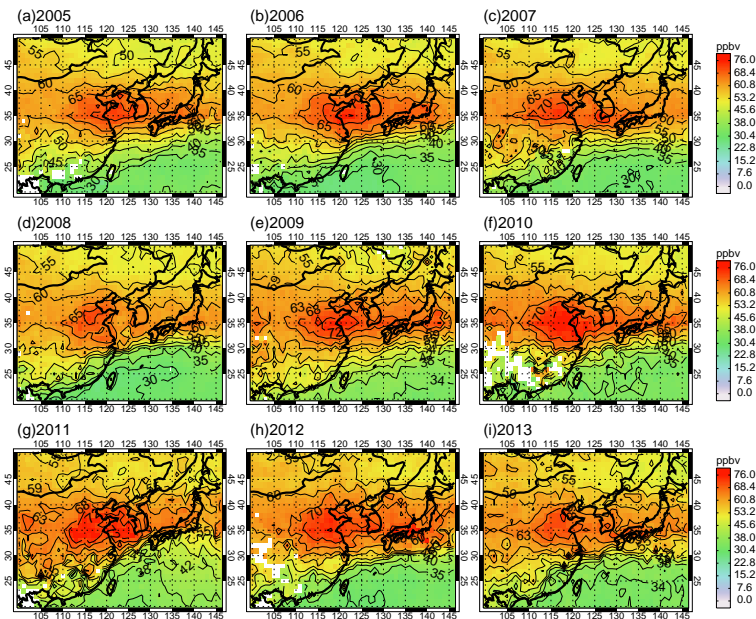


Figure 12. Maps of monthly mean of retrieved ozone at the 24th layer in June from 2005 through 2013.

[Title Page](#)[Abstract](#)[Introduction](#)[Conclusions](#)[References](#)[Tables](#)[Figures](#)[◀](#)[▶](#)[◀](#)[▶](#)[Back](#)[Close](#)[Full Screen / Esc](#)[Printer-friendly Version](#)[Interactive Discussion](#)